Bioorganic & Medicinal Chemistry Letters 19 (2009) 557–583

Contents lists available at ScienceDirect

Bioorganic & Medicinal Chemistry Letters

journal homepage: www.elsevier.com/locate/bmcl

Bioorganic & Medicinal Chemistry Letters Vol. 19, No. 3, 2009

Contents

ARTICLES

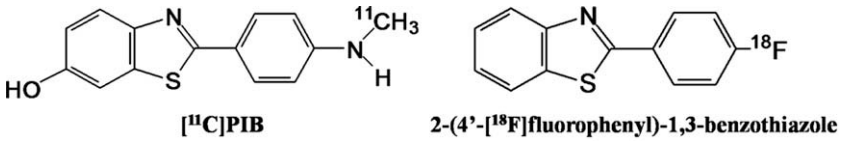

[^{11}C]PIB 2-(4'-[^{18}F]fluorophenyl)-1,3-benzothiazole

2-(4′-[^{18}F]Fluorophenyl)-1,3-benzothiazole was synthesized as derivative of [^{11}C]PIB to overcome the limitations associated with the short half-life of the carbon-11 label and was biologically evaluated in comparison with PIB.

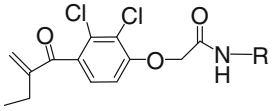

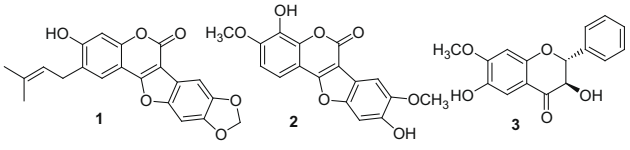

Three new compounds named buteaspermin A (**1**), buteaspermin B (**2**) and buteaspermanol (**3**), along with 19 known compounds were isolated from the stem bark of *Butea monosperma*. Five of these compounds **7**, **10**–**13** showed promising osteogenic activity.

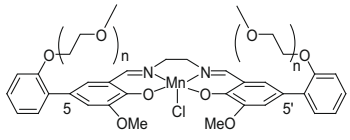

n = 1, 2, 3, 4, 6, 8

The SOD activities of oligo(ethylene glycol) derivatives of manganese salen complexes were similar and slightly more potent than the standard compound EUK-134. Their catalase-like activity was lower than that of EUK-134 in the initial conversion rate; however, some analogs exhibited a better catalytic turnover number.

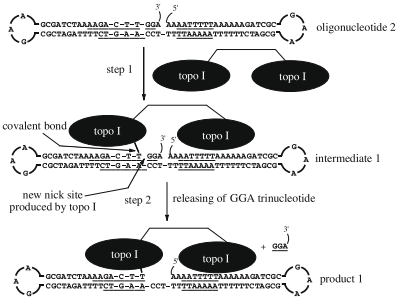

Here, we report oligonucleotides with various lengths that contain nick and topoisomerase I-binding sites as human topoisomerase I inhibitors.

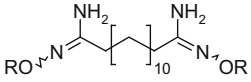

Specific *O*-substitutions of amidoximes are needed to design orally potent *C*-alkylamidine-based antimalarial agents.

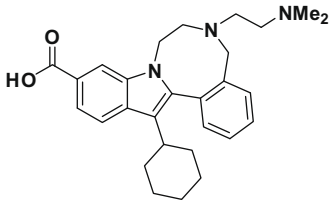

The evolutionary path is reported to conformationally constrained indole inhibitors of HCV NS5B-polymerase. Biochemical and cell-based potency was achieved, coupled with attractive DMPK properties—leading ultimately to the identification of a pre-clinical candidate with an excellent predicted human pharmacokinetic profile.

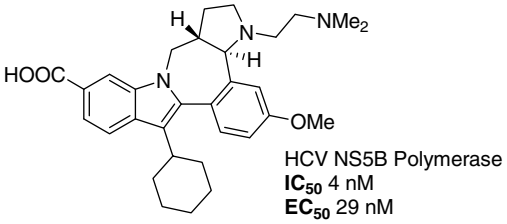

The synthesis and SAR of pentacyclic indoles as potent inhibitors of HCV NS5B polymerase is reported.

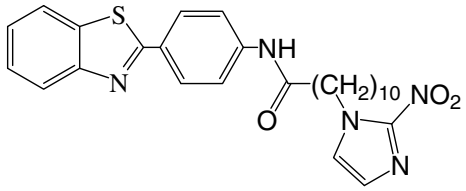

2NUBTA

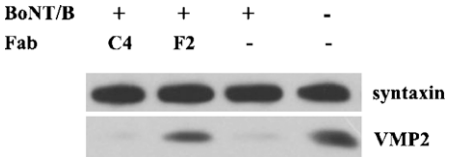

A human neutralizing antibody was selected from a naïve phage display library that specifically binds Botulinum neurotoxin serotype B. Biochemical studies provide evidence for its therapeutic potential and further development.

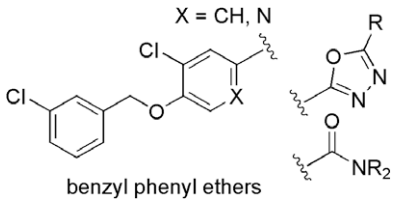

benzyl phenyl ethers

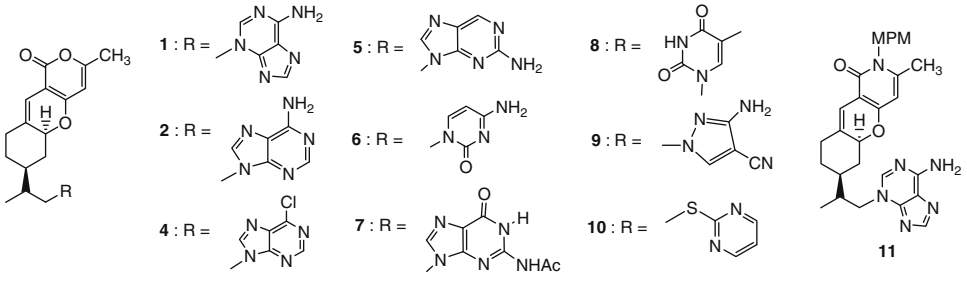

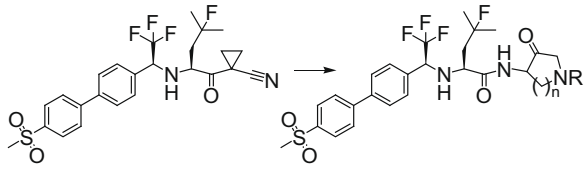

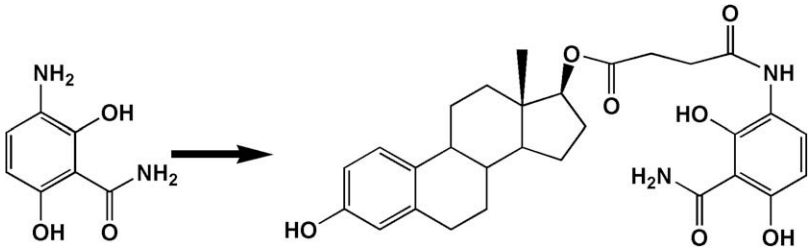

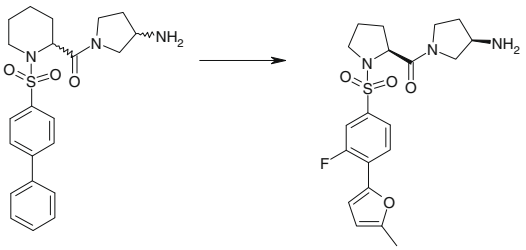

(**2**) GHSR pEC50 (IA) 7.5 (0.8)
mixtures of diastereomers

(**19**) GHSR pEC50 9.4 (1.2)
orally bioavailable

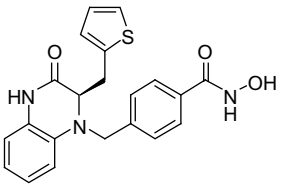

7d
HDAC6 IC_{50} = 40 nM
EC_{50} TubAc = 70 nM

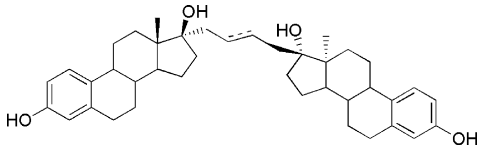

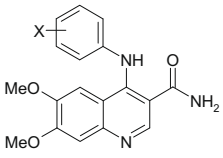

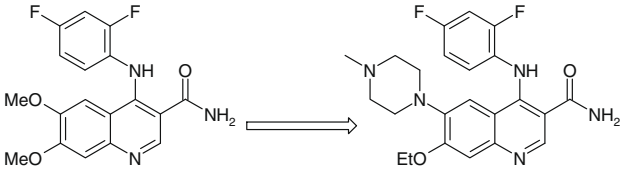

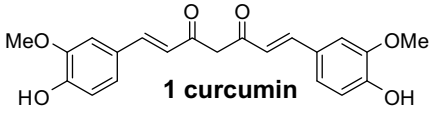

A potent dietary DNA methylation inhibitor, curcumin **1** (EC_{50} = 30 nM) and its hypomethylation activity on MV4-11 cells (15–20% decrease in global DNA methylation) is reported.

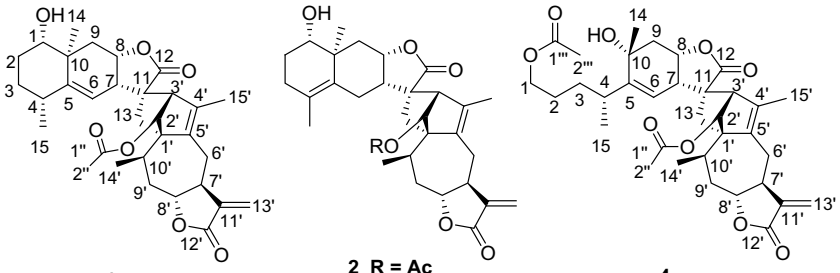

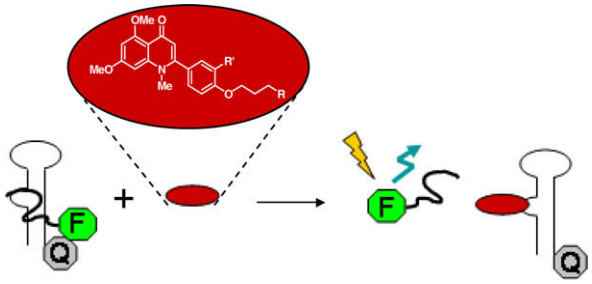

Fluorescence quenching analysis demonstrates that 2-phenylquinolone derivatives efficiently inhibit Tat/TAR recognition.

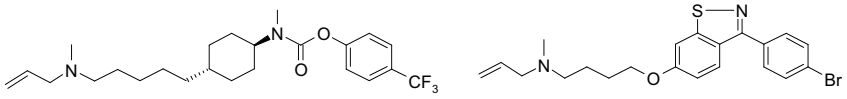

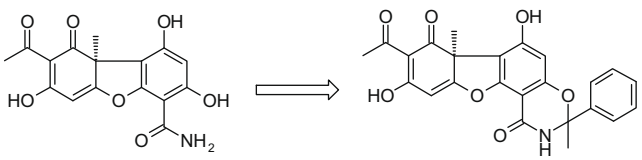

The synthesises of (−)-Cercosporamide derivatives and their plasma glucose lowering effects are reported.

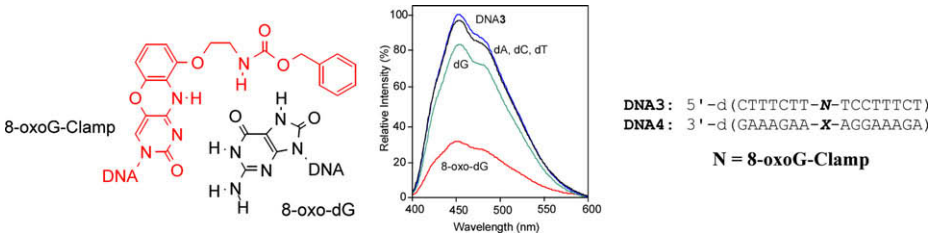

The 8-oxoG-clamp, a specific fluorescence probe for 2′-deoxy-8-oxoguanosine (8-oxo-dG) in solutions, was incorporated into the ODN, which was shown to be a selective fluorescence probe for 8-oxo-dG in DNA.

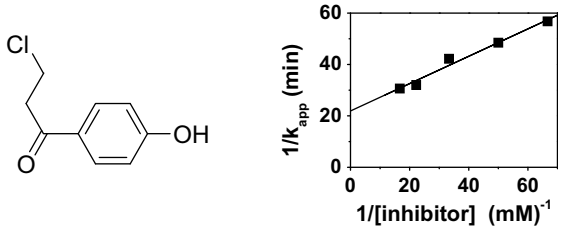

3-Chloro-1-(4-hydroxyphenyl)propan-1-one (**9**) was found to inactivate potently the enzyme in a time-dependent manner.

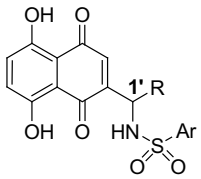

2 R=*i*-Pr
3 R=Me

A series of shikonin analogues have been synthesized, these new analogues showed substantial in vitro antitumor activity.

Riccardin C and its 7 analogues were synthesized. The structure–activity relationship of these compounds indicated that all hydroxy groups in riccardin C are essential for its binding to LXRα.

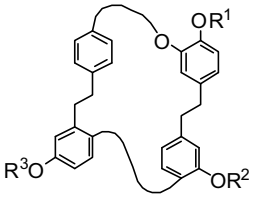

R^1 - R^3 = H : riccardin C
R^1 - R^3 = H or Me:
7 possible analogues

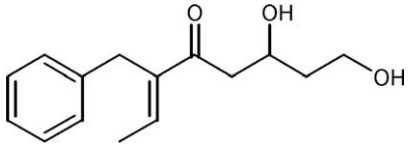

The chemical structure and nomenclature of F3-2-5, (*E*)-3-benzyl-6,8-dihydroxyoct-2-en-4-one.

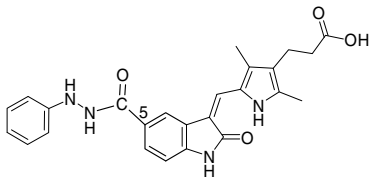

NP506

The introduction of the phenyl hydrazide motif to the position 5 of the pyrido[2,3-*d*]pyrimidine scaffold in NP506 led to the inhibitory effect in two signaling pathway: inhibition of AKT activation in the phosphatidyl inositol 3′-kinase (PI13K)/AKT signaling pathway and the inhibition of ERK and JNK activation in MAPK pathway.

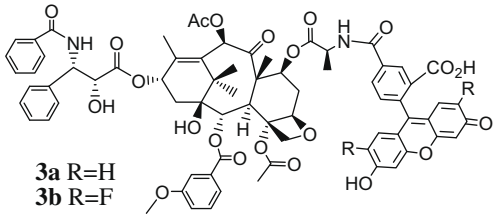

3a R=H
3b R=F

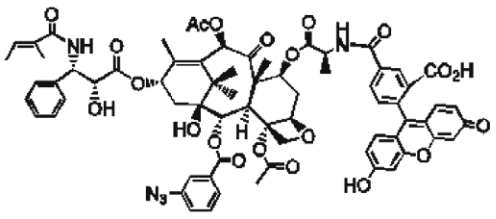

4

Three fluorescent probes **3a**, **3b**, and **4** have been synthesized through conjugation of fluorescein and difluorescein groups to the 7-OH of C-2 modified paclitaxel and cephalomannine derivatives with very high affinity to microtubules. All these probes exhibited potent tubulin assembly promotion and tumor cell killing activities.

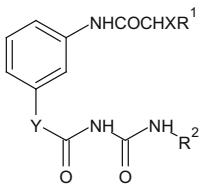

X = Cl, Br; R^1 = H, CH_3; Y = CH_2, CH=CH;

R^2 = methyl, phenyl, 3,4,5-trimethoxyphenyl, 3,4-methylenedioxyphenyl, 2-pyridyl

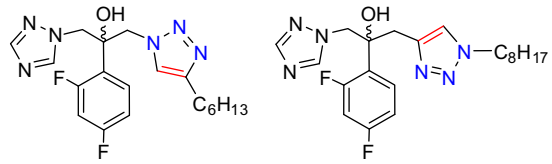

Fluconazole analogues

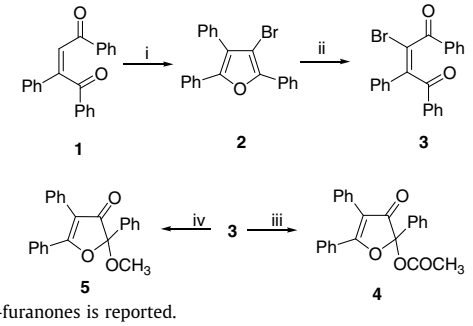

Synthesis and antitumor activity of two triaryl-3(2*H*)-furanones is reported.

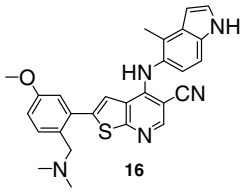

The 4-(4-methyl-1*H*-indol-5-ylamino)thieno[2,3-*b*]pyridine-5-carbonitrile **16** had an IC_{50} of 16 nM for the inhibition of PKCθ activity.

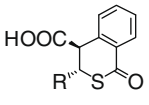

2
R= alkyl

The synthesis and biological activity of a new series of compounds **2** are described.

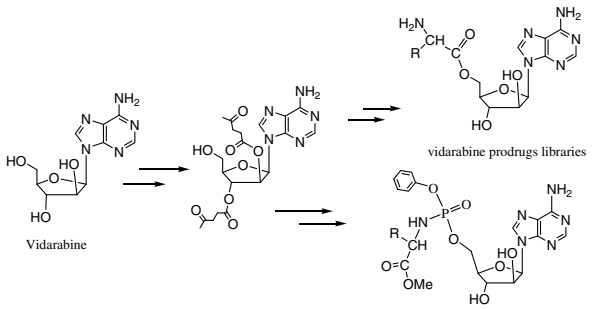

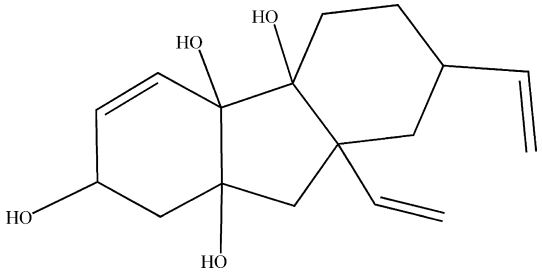

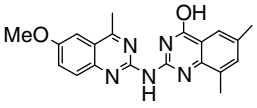

30, IC_{50} = 0.3 μM , MIC = 0.25 μg/mL

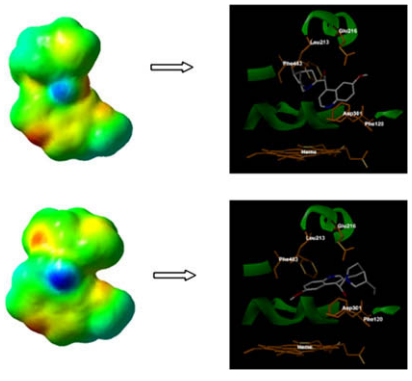

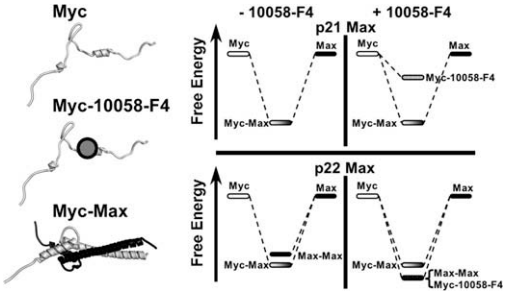

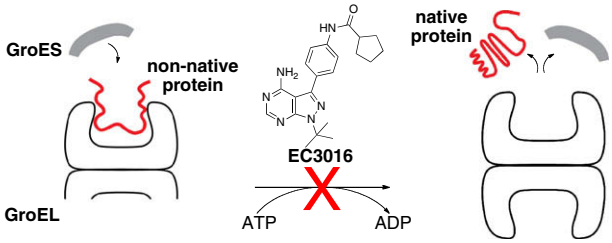

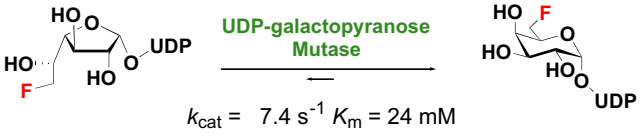

Two new series of potent and selective dual EGFR/ErbB-2 kinase inhibitors derived from novel thienopyrimidine cores have been identified. Isomeric thienopyrimidine cores were evaluated as isosteres for a 4-anilinoquinazoline core and several analogs containing the thieno[3,2-*d*]pyrimidine core showed anti-proliferative activity with IC_{50} values less than 1 μM against human tumor cells in vitro.

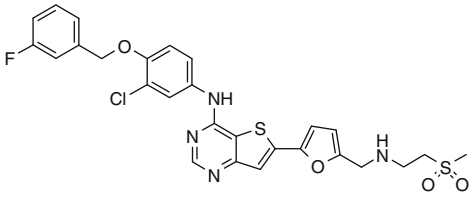

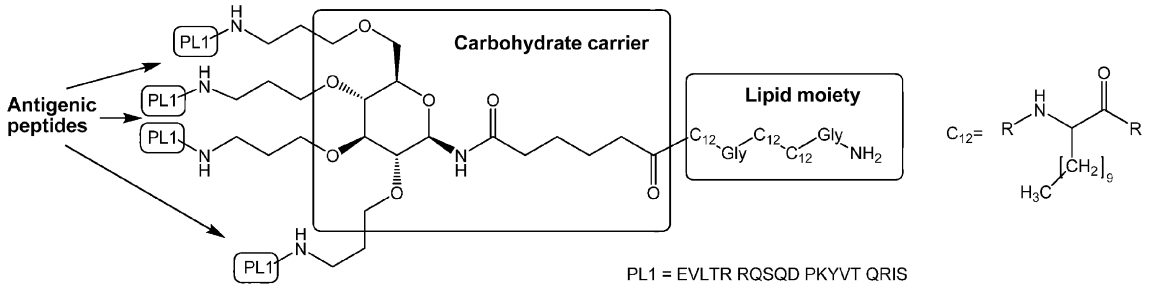

A complex vaccine candidate against group A streptococcus incorporating carrier, adjuvant and the antigen was synthesised using carbohydrate chemistry and solid-phase peptide methods.

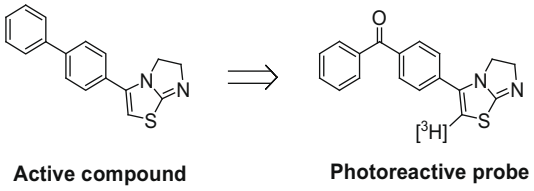

The synthesis of a radiolabeled photoreactive probe to elucidate the mechanism of transmembrane iodide fluxes in the thyroid gland is reported.

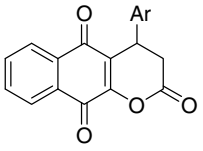

The synthesis of α-lapachone derivatives as new potential inhibitors of DNA topoisomerase II is reported.

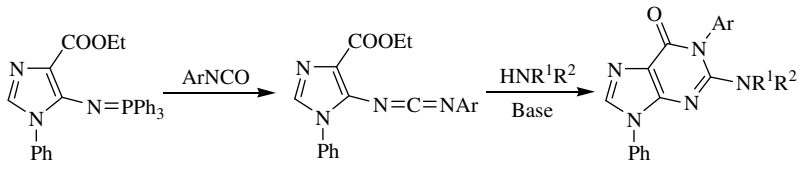

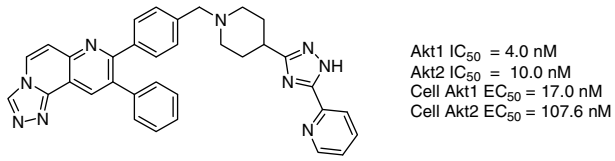

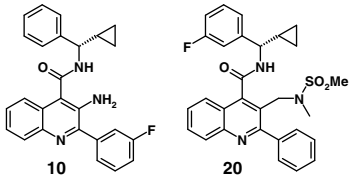

SAR investigation in the quinoline series of NK_3 antagonists led to identification of 3-amino quinoline **10** (GSK172981) and sulfonamide **20** (GSK256471). Both compounds are high affinity, potent NK_3 receptor antagonists which produce excellent NK_3 receptor occupancy in an ex vivo binding study in gerbil cortex.

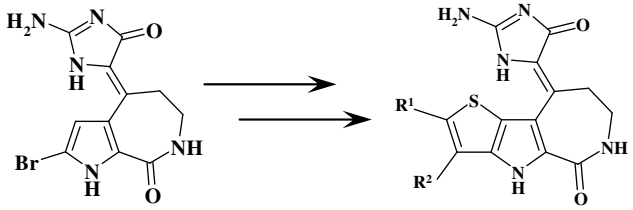

Hymenialdisine

Thieno[3,2-*b*]pyrroloazepinones analogues of Hymenialdisine were prepared and found to be potent inhibitors of CHK1.

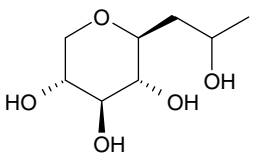

Pro-Xylane™

The scope and limitation of Lubineau's reaction were evaluated for the synthesis of C-glycosides. Further transformation of side chain carbonyl was also achieved. Optimization of these two steps was investigated in xylose case. Some of the compounds were shown to stimulate sulfated glycosaminoglycans (GAGs) synthesis. Pro-Xylane™ was identified as the best activator of GAGs biosynthesis.

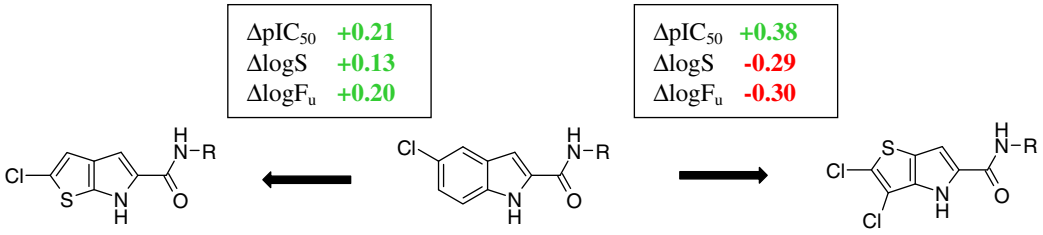

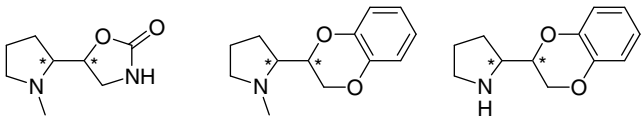

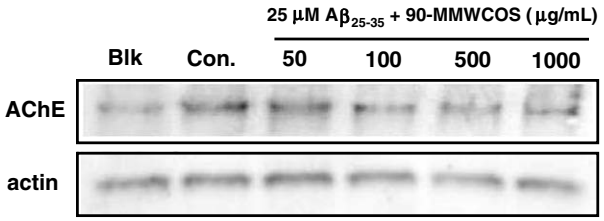

A 90-MMWCOS (MW 1000–5000Da) suppressed the level of AChE protein expression and AChE activity induced by $A\beta_{25-35}$ in PC12 cell lines.

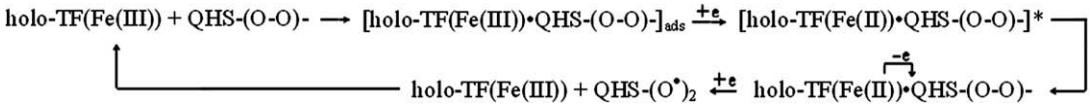

A sequential two-step process is proposed to explain hololtransferrin-mediated electrocatalytic reduction of artemisinin. Holotransferrin (holo-TF) initially interacts with artemisinin (QHS) to form an adduct [holo-TF(Fe(III))·QHS–(O–O)–]$_{ads}$, subsequently, holo-TF(Fe(III)) obtains one electron and then forms an intermediate adduct [holo-TF(Fe(II))·QHS–(O–O)–]*, which induces the cleavage of the peroxide bond in artemisinin and then generates QHS-(O$^{\bullet}$)$_2$ free radicals.

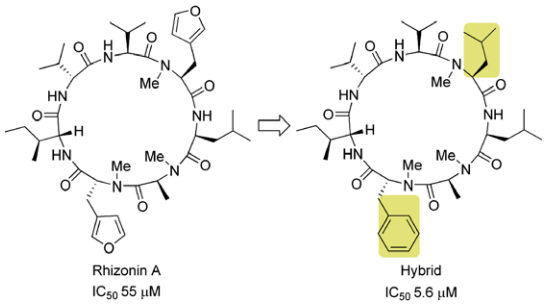

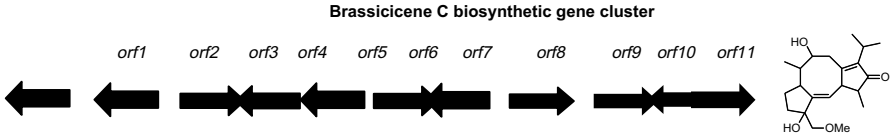

The biosynthetic gene cluster of brassicicene C was identified in *Alternaria brassicicola* strain ATCC 96836 from genome database search.

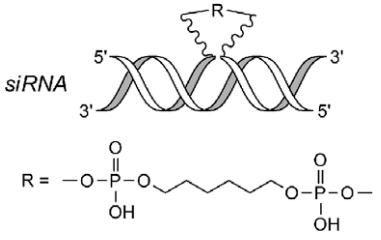

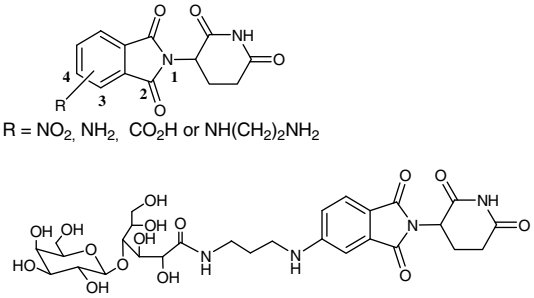

Synthesis and biological assessments in vitro (on EAhy926 cells) and in vivo (EAE model) of new thalidomide analogues.

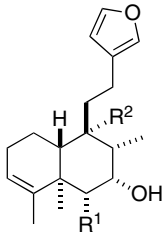

1 R^1 = OH, R^2 = CH_3
2 R^1 = H, R^2 = CH_2OH

Among four novel clerodane-type diterpenoids **1**–**4** isolated from *Ptychopetalum olacoides*, **1** and **2** were found to significantly enhance neurite-outgrowth of NGF-differentiated PC12 cells at 0.1–50 μM.

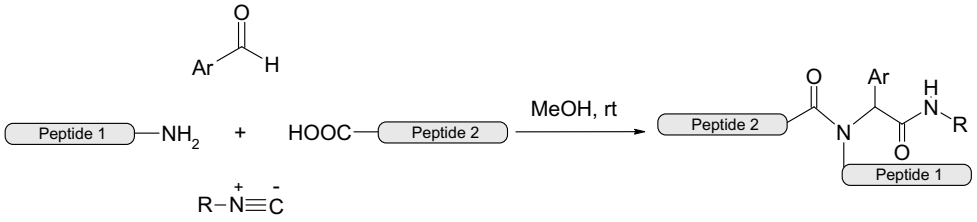

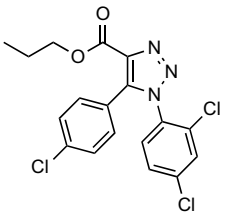

A series of 4-alkoxycarbonyl-1,5-diaryl-1,2,3-triazoles were synthesized regioselectively using click chemistry and evaluated at CB1 cannabinoid receptors. The *n*-propyl ester (K_i = 4.6 nM) exhibited the most potent affinity of the series.

The synthesis and antibacterial activities of three chemotypes of DNA supercoiling inhibitors based on imidazolo[1,2-*a*]pyridine and [1,2,4]triazolo[1,5-*a*]pyridine scaffolds that target the ATPase subunits of DNA gyrase and Topoisomerase IV (GyrB/ParE) is reported. The most potent scaffold was selected for optimization leading to a series with potent Gram-positive antibacterial activity and a low resistance frequency.

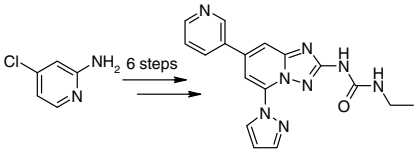

GyrB IC_{50} 54 nM
MICs 2-4 μg/ml (Gram +ve)

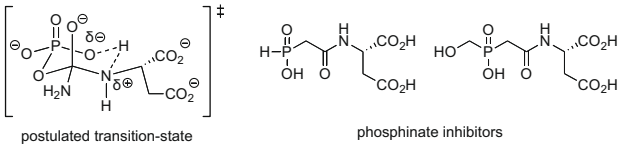

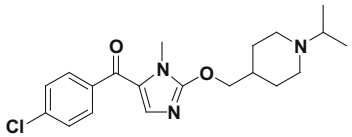

22
hH_3 K_i = 3 nM
hpA_2 = 9.2

A novel series of imidazole containing histamine H_3 receptor ligands were Investigated and found to be potent functional antagonists with appreciable brain uptake.

The design and synthesis of a potent and isoform selective PKCw-ζ (**9**, IC_{50} = 5.2 nM, 10- to 20,000-fold selective over other PKC isoforms, 200-fold selective over CDK-2) inhibitor is reported.

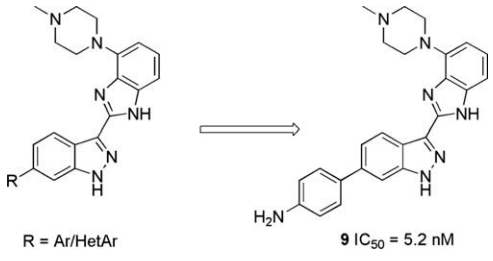

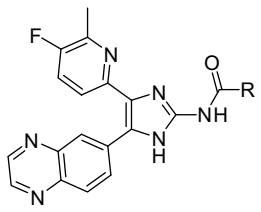

Acylated 2-amidoimidazoles were identified as potent and selective inhibitor of TGF-βR1 that offer a superior pharmacokinetic profile compared to unsubstituted or alkylated 2-aminoimidazoles.

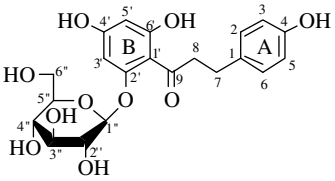

Phloridzin

The synthesis and [^{3}H]-uridine uptake investigation of the structure–activity relationship of new phloridzin analogs at the human concentrative nucleoside transporter 3 (hCNT3) is reported.

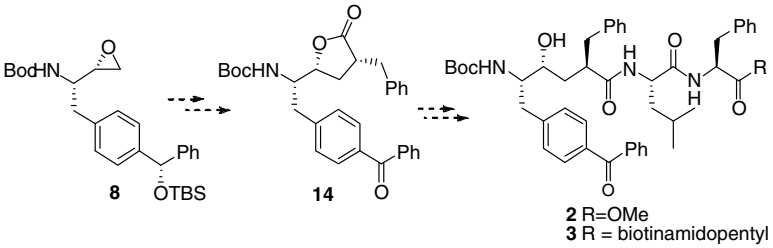

Synthesis of a photoreactive dipeptide isostere at the P1 position.

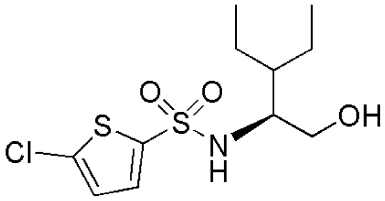

7.b.2

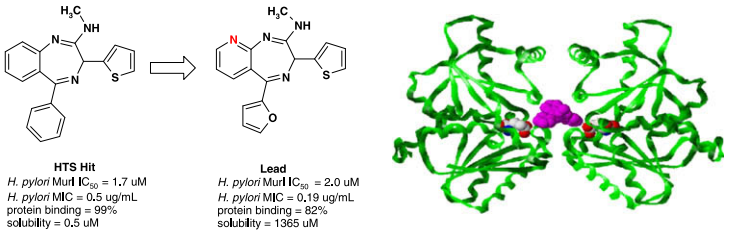

An SAR study of a screening hit generated a series of pyridodiazepine amines as inhibitors of *Helicobacter pylori* glutamate racemase (MurI) showing highly selective anti-*H. pylori* activity, marked improved solubility, and reduced plasma protein binding. X-ray co-crystal E–I structures were obtained. These uncompetitive allosteric inhibitors bind at the MurI dimer interface.

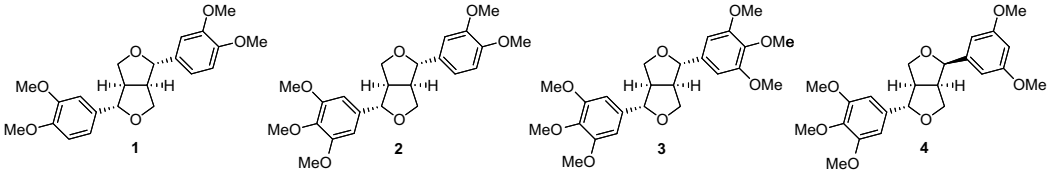

Lignans from *Magnolia fargesii* inhibit the production of NO, PGE_2 and expression of iNOS and COX-2 by activated microglia.

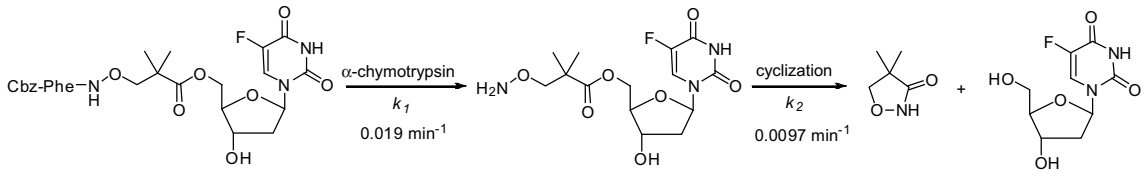

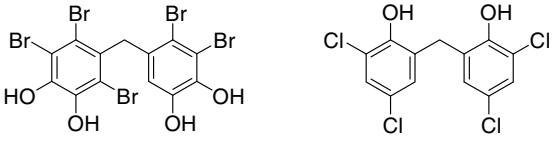

The synthesis and bioactivity of halophenols are described.

A number of spiro[chroman-2,4′-piperidin]-4-one derivatives (**38a**–**m** and **43a**–**j**) have been designed, synthesized and screened for in vitro ACC inhibition. In vivo studies of compound **38j** has been carried out.

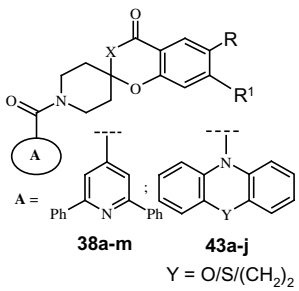

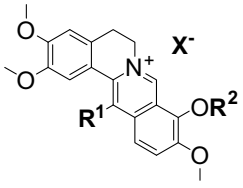

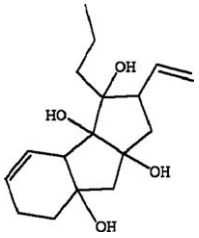

The chemical structure of HY251 3-propyl-2-vinyl-1,2,3,3a,3b,6,7,7a,8,8a-decahydrocyclopenta[*a*]indene-3,3a,7a,8a-tetraol.

The synthesis and SAR of two mGluR4 positive allosteric modulator leads **6** and **7** is described. VU001171 (**6**) represents the most potent (EC_{50} = 650 nM), efficacious (141% Glu Max) and largest fold shift (36-fold) of any mGluR4 PAM ever described. However, this work highlights the challenges in hit-to-lead for mGluR4 PAMs, with multiple confirmed HTS hits displaying little or no tractable SAR.

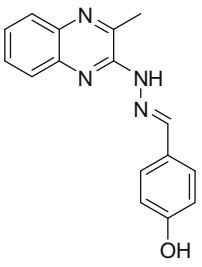

VU0001171, **6**

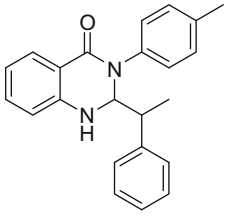

VU0092145, **7**

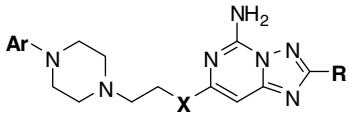

1

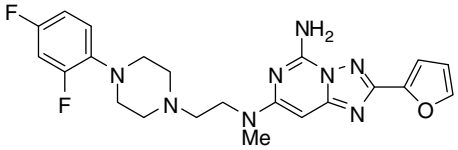

16g A_{2A} Ki = 1.0nM, A_1/A_{2A} = 1580 X

Synthetic methodology was developed for a series of 1,2,4-triazolo[1,5-*c*]pyrimidines of type **1**. These compounds, exemplified by **16g**, showed potent and selective adenosine A_{2A} antagonist activity, as well as oral activity in a rodent model of Parkinson's disease.

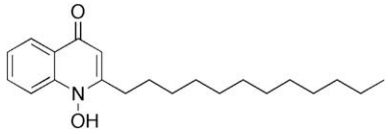

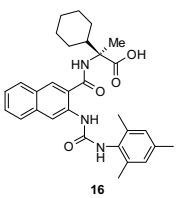

16
IC_{50} (+glu) = 10 nM
IC_{50} (cell) = 350 nM
CYP2C9 IC_{50} = 9,200 nM
37 %F (rat)

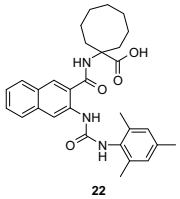

22
IC_{50} (+glu) = 5 nM
IC_{50} (cell) = 498 nM
CYP2C9 IC_{50} > 33,000 nM
28 %F (rat)

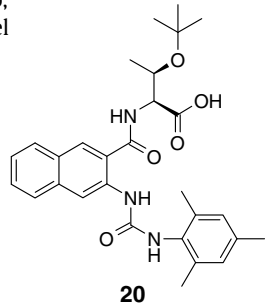

20

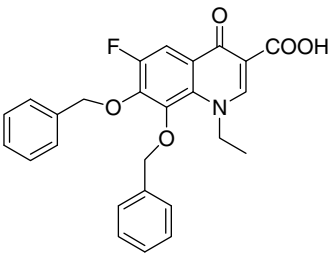

10, IC_{50} = 1.3 μg/mL

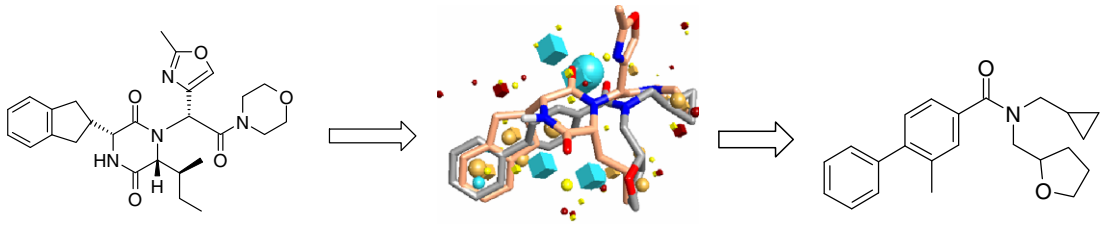

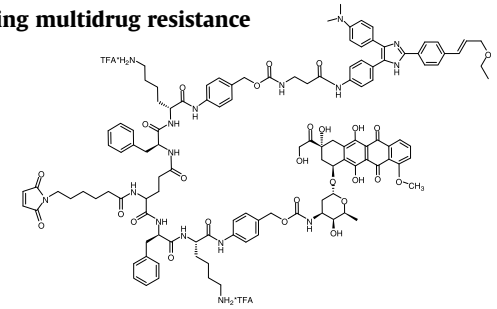

We have developed a novel dual-acting maleimide-bearing prodrug that incorporates the anticancer agent doxorubicin and an inhibitor of the P-glycoprotein efflux pump that is over-expressed in multidrug resistant tumor cells. Additionally, the prodrug contains a 1,6-self-immolative spacer coupled to the dipeptide Phe-Lys that acts as a substrate for cathepsin B. The prodrug, once bound through its maleimide moiety to the cysteine-34 group of human serum albumin, was cleaved by cathepsin B and in tumor homogenates demonstrating a release of the anticancer agent doxorubicin and the inhibitor.

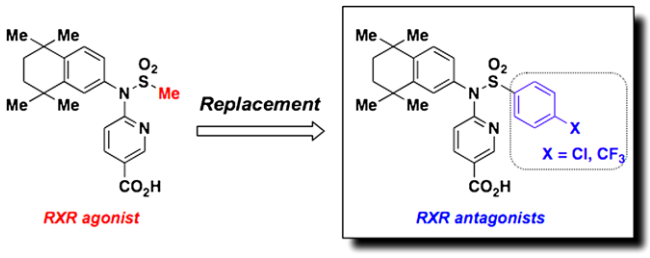

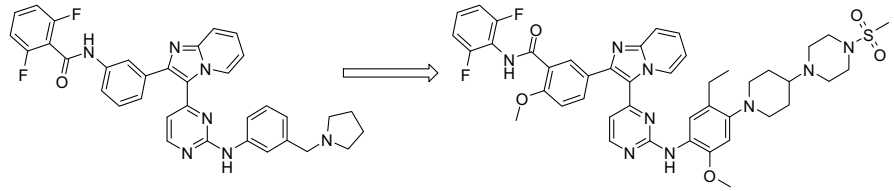

IGF-1R IC_{50} = 180 nM
IGF-1R Cellular IC_{50} = 5930 nM

IGF-1R IC_{50} = 27 nM
IGF-1R Cellular IC_{50} = 22 nM

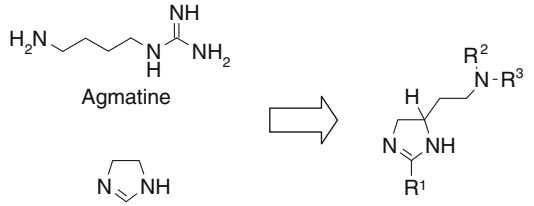

The synthesis and α_2, I_1, and I_2 receptors' affinity studies of new agmatine analogues are reported.

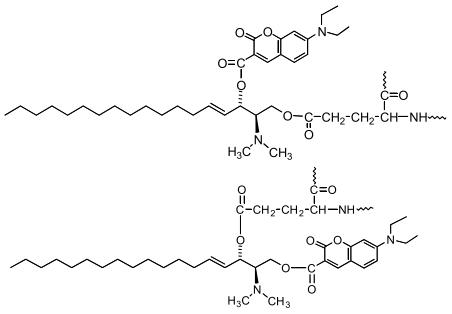

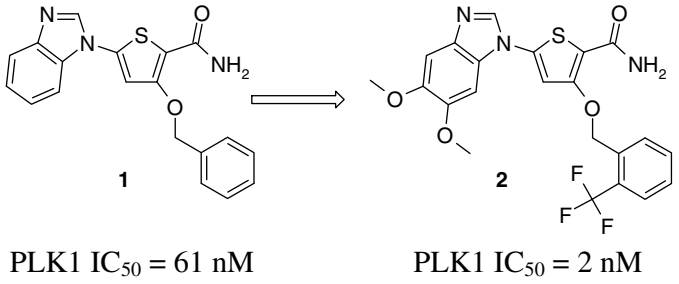

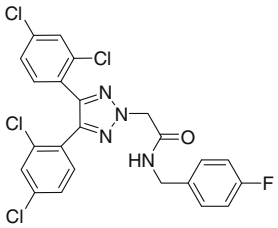

Development of new 1,2,3-triazoles as effective and selective CB1 receptor antagonists (IC_{50} = 11.6 ± 3.4 nM; CB2/CB1 > 1000) is reported.

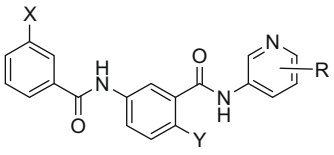

Potent amidoheteroaryls inhibitors of V600E B-Raf with in vivo activity.

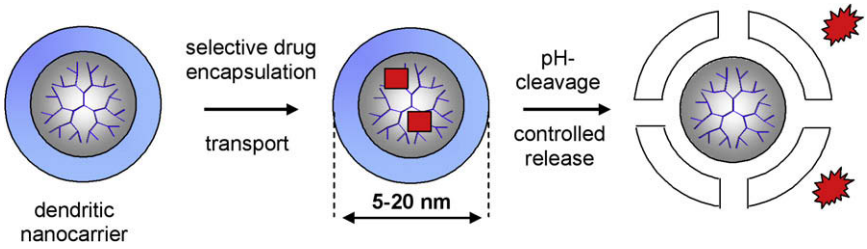

OTHER CONTENTS

*Corresponding author
Supplementary data available via ScienceDirect

COVER

Overlay of high resolution co-crystal structures of *R*-**22**-ADP (cyan) and **1**-ADP (green) bound in an allosteric binding site of the mitotic kinesin KSP. [Roecker, A. J.; Coleman, P. J.; Mercer, S. P.; Schreier, J. D.; Buser, C. A.; Walsh, E. S.; Hamilton, K.; Lobell, R. B.; Tao, W.; Diehl, R. E.; South, V. J.; Davide, J. P.; Kohl, N. E.; Yan, Y.; Kuo, L. C.; Li, C.; Fernandez-Metzler, C.; Mahan, E. A.; Prueksaritanont, T.; Hartman, G. D. *Bioorg. Med. Chem. Lett.* **2007**, *17*, 5677.]

Indexed/Abstracted in: Beilstein, Biochemistry & Biophysics Citation Index, CANCERLIT, Chemical Abstracts, Chemistry Citation Index, Current Awareness in Biological Sciences/BIOBASE, Current Contents: Life Sciences, EMBASE/Excerpta Medica, MEDLINE, PASCAL, Research Alert, Science Citation Index, SciSearch, TOXFILE

ELSEVIER

ISSN 0960-894X